Engineering Structures 32 (2010) 911–921

Contents lists available at ScienceDirect

Engineering Structures

journal homepage: www.elsevier.com/locate/engstruct

The vulnerability of residential window glass to lightweight windborne debris

Forrest J. Masters *, Kurtis R. Gurley [1], Nirav Shah, George Fernandez

Department of Civil and Coastal Engineering, University of Florida, 365 Weil Hall, Gainesville, FL 32611, United States

ARTICLE INFO

Article history:
Received 1 September 2009
Received in revised form
3 December 2009
Accepted 5 December 2009
Available online 13 February 2010

Keywords:
Windborne debris
Missile impact
Vulnerability curve
Branch
Shingles
Glass

ABSTRACT

This paper presents the results of an experimental investigation of the momentum threshold required to damage residential window glazing when impacted by roof shingles and wooden dowels. Shingles are among the most common sources of debris in hurricane winds, and they have been observed to be a major contributor to the breach of windows. Wooden dowels represent lightweight vegetation type windborne debris (e.g., twigs, branches). Custom launching apparatuses were constructed to achieve controllable and repeatable flight modes and speeds for the debris. More than 600 annealed residential window glass specimens were tested to quantify the momentum threshold and damage accumulation. The shingle impact experiments were conducted using varying shingle sizes, flight modes, impact angles, shingle age, impact speeds, glass specimen thicknesses, dimensions, and edge boundary conditions. The wooden dowel impact experiments include varying wooden dowel diameters and angles of impact. Vulnerability curves are provided for unprotected window glass as a function of momentum, debris type, flight mode, and angle of impact.

Published by Elsevier Ltd

1. Introduction

Windborne debris can cause significant damage to building envelopes in high wind events. Building codes along the hurricane prone US coast have evolved to address debris impact on the building envelope, requiring the testing of fenestration, wall and roof claddings in order to certify a minimum impact resistance standard. For the purpose of maintaining a repeatable procedure with controlled representative impact momentum, these standards (e.g., [1–3]) specify testing with 2 × 4 (inch) lumber and/or steel balls as the debris source [4].

Methods to investigate building vulnerabilities, to model probable losses on an event-wide level, and to determine the cost effectiveness of various mitigation measures are evolving, based in part on experimental research. These methods can benefit from specific information about the capability of various debris materials to damage the building envelope. For example, risk models that project losses from hurricane winds address the vulnerability of both protected and unprotected glazed openings to windborne debris [5,6]. The likelihood of damage to openings caused by commonly observed debris such as roof cover and vegetation is a relevant quantity, allowing the inclusion of building and tree density, prevalent local roof cover type, etc. as modeling variables.

Several recent post-storm investigation studies have noted a high degree of roof cover loss, particularly for aged roof systems (e.g. [7–10]), indicating that roof cover is a primary source of potentially damaging windborne debris in residential areas. To date there is a dearth of statistical information regarding the vulnerability of unprotected residential window glass subjected to debris typically observed in post-storm field studies.

Double-strength (3.18 mm thickness) annealed glass is one of the most common glazing materials used in residential window panes and is the test subject in this study. Annealed glass is a brittle substance with low toughness and ductility. For the purposes of determining vulnerability to impact loading, experimental evaluation is necessary, as the theoretical strength can differ greatly from the measured strength due to surface flaws imparted during the manufacturing process (see [11] for a review of the fracture mechanics of glass).

This paper presents the results of an experimental investigation of the momentum threshold required to damage typical annealed residential window glazing when impacted by (a) roof shingles and (b) wooden dowels. All testing was conducted at the Powell Family Structures and Materials Testing Laboratory on the Eastside Campus of The University of Florida (UF). Testing apparatus were constructed to allow a controllable and repeatable flight mode and speed for the debris. More than 600 samples of annealed residential window glass were tested following a protocol designed to extract information regarding momentum threshold and damage accumulation via repeated impacts. Experimental variables included two shingle sizes, spinning and tumbling flight modes, 45° and 90° impact angles, new shingles and

* Corresponding author. Tel.: +1 352 392 9537x1505.
E-mail addresses: masters@ce.ufl.edu (F.J. Masters), kgurl@ce.ufl.edu (K.R. Gurley).
[1] Tel.: +1 352 392 9537x1508.

0141-0296/$ – see front matter. Published by Elsevier Ltd
doi:10.1016/j.engstruct.2009.12.016

naturally aged shingles, and a range of impact speeds. Two different glass specimen thicknesses, dimensions, and edge boundary conditions were tested. The wooden dowel impact experiments include 2.4 cm (1 in) and 5.08 cm (2 in) diameter wooden dowels, two angles of impact, and one size and thickness of glass. The experimental results were evaluated to provide a series of vulnerability curves for unprotected window glass as a function of momentum. Analysis of variance (ANOVA) and Welch's t tests were performed on the experimental data to evaluate the influence of debris type and size, flight mode, glass specimen size and edge boundary conditions, and angle of impact.

2. Prior research

Post-hurricane damage research cites windborne debris as a common source of damage to the building envelope. Minor [4] recorded observations during various windstorm events and presented a synopsis of damage observations for various hurricanes such as Celia (1970), Frederic (1979), Allen (1981), Alicia (1983), and Andrew (1992). Beason [12] investigated the damage caused by Hurricane Alicia (1983) in Houston, Texas, and observed that windborne missiles from building roofs were the major cause of damage to architectural glazing systems. Following Hurricane Andrew (1992), Oliver and Hanson [13] observed that debris impact shattered glazing components. Roofing materials were the most common type of debris that caused damage to building envelope systems [14].

In the investigations following Hurricane Charley in 2004, researchers found that a principal source of windborne debris was ridge shingles. The loss of tiles along eaves, hips and ridges were also documented [8–10]. In many cases windows were broken by debris originating from a neighbor's house [10]. Gurley [7] provided statistics on window performance during the 2004 storms as related to wind speed, window protection use, and the dominant local roof cover type.

Numerous studies have been conducted on the impact resistance of annealed/tempered glass [15,16] and laminated glass [17–21]. Variation of the target's surface area has been shown to have little effect on the mean minimum breaking velocity [22,23]. Minor [24] found that the presence of a uniform wind pressure on the glazing affects the character of the breakage but does not lower the missile speed required to break glass.

Beason [15] investigated the breakage characteristics of glass specimens when subjected to small missile impacts. Test specimens of two thicknesses were subjected to missile impacts from steel balls representative of roof gravel debris. Missile size was determined to be a significant factor for the breakage of glass, and 6.35 mm (1/4 in) glass was found to be as vulnerable to missile impact damage as 2.38 mm (3/32 in) glass. Harris [16] conducted tests on 257 samples of annealed, heat tempered and fully tempered glass of varying thickness to determine the gravel impact velocities required to break glass, and concluded that missile mass was the most important damage indicator. Bole [25] tested annealed, heat strengthened, and tempered glass using 2 × 4 timber missiles of 2.0 kg (4.5 lb), 4.1 kg (9 lb), and 8.2 kg (18 lb), and found that missiles of different mass but the same kinetic energy produced different results. Other related studies include [26–28].

The only published study quantifying the resistance of annealed glass to impact from asphalt composite shingles was performed by the National Association of Home Builders Research Center (NAHB) [23], and it found that the resistance of the glass increased proportionally with glass thickness. The NAHB study impacted glass with rolled bundles of shingles. This configuration differs from the natural state of loose shingles as observed in high wind environments and can potentially alter the dynamics of impact rather significantly via energy dissipation through shingle deformation. In contrast, the current study replicates two shingle flight modes representative of field conditions. The NAHB study also used 2 × 4 missiles of 2 kg, whereas the current study uses 200 g 2.54 cm and 5.08 cm diameter dowels, which were selected to be representative of lightweight vegetation rather than construction material.

2.1. Debris models

The work in this study is intended to complement recent advances in debris flight and impact probability modeling with reliable test data quantifying the vulnerability of glazing to debris typical of the hurricane environment. Twisdale et al. [29,30] developed a windborne debris model to estimate the impact risk in residential environments that accounts for residential roof debris. The kinetic energy and momentum of the debris are calculated and used to project the probability of damage to openings. Lin and Vanmarcke [31] proposed a Poisson-based probabilistic model of debris impacting individual buildings and communities.

Wills [32] developed a debris model based on the assumption that the amount of damage sustained is proportional to the missile kinetic energy. Holmes [33,34] developed a theoretical flight model for several idealized debris shapes. Additional wind-tunnel experiments and numerical simulations of debris flight behavior include [35–38]. Kordi and Kopp [39] recently completed a series of wind tunnel experiments to study debris flight upon release from a sloped roof.

3. Summary of methods

Experiments were conducted to elicit the influence of numerous controlled variables, including thickness, size, and edge restraints of the glass specimens, along with material type, size, angle of impact, momentum, and flight mode of impacting debris. The methodology included development of debris launching apparatus, specimen restraint, test protocol, and test matrix of debris and glass specimen types. Three phases of tests were conducted.

- Phase 1 determined the dependence of the breakage momentum on the shingle size, flight mode, glass specimen size, and other parameters described later.
- Phase 2 developed vulnerability curves for one size and thickness of glass, one shingle size, two angles of impact and two flight modes.
- Phase 3 developed vulnerability curves for one size and thickness of glass, two dowel sizes, and two angles of impact.

Phase 1 was conducted in the summer and fall of 2008, and Phases 2–3 were carried out in the spring of 2009. The following sections describe the experimental apparatus, test protocols, and results and analysis of each phase.

4. Simulation of shingle impacts (Phases 1 and 2)

4.1. Description of testing apparatus

Phases 1 and 2 used a shingle launching apparatus designed to propel asphalt shingles over a short distance into a glass specimen. It consists of two vertically oriented rubber tires of 0.20 m radius contacting each other at the treads. A 0.75 kW (1 hp) Franklin Electric AC induction motor spins the bottom tire, which causes the top tire to contra-rotate (Fig. 1). Shingles are fed into the contact region and are propelled toward the target. A motor controller allows the angular velocity of the tires to be adjusted from 250 to 1450 RPM.

By rotating and tilting the launcher, the flight dynamic of the shingle can be controlled to produce spinning (the shingle plane

Fig. 1. Shingle launching apparatus.

is horizontal, and rotation is about the vertical axis) or tumbling (the initial shingle plane is horizontal, and rotation is about the horizontal axis perpendicular to the flight path) modes of flight.

The speed of the airborne shingle is related to the tangential speed of the wheels by a proportionality constant that was experimentally determined by comparing the motor RPM to video tracking of the shingle using a 1000 fps high speed camera. This constant varied from 0.70 to 0.98 depending upon the specific experiment (shingle size and flight mode). Over the range of speeds used in the study, the constant was not found to be a function of RPM.

A 1.4 m deep × 1.2 m wide × 2.4 m tall wood frame box sheathed in 1.3 cm plywood was built to house the glazing support frame and to contain the broken glass. On the side facing the shingle launcher, the specimen box has a 1.0 m wide × 1.1 m high opening through which the shingle passes (Fig. 1). A support frame restrained glass specimens of varying thickness and size inside the box. Glass specimens were clamped in place using continuous steel brackets with weather-stripping at the contact interface. The frame accommodated either a four-sided glass restraint or a two-sided (top and bottom) restraint.

4.2. Testing protocols

The protocols differed between Phases 1 and 2, and are respectively referred to as Protocol A and B. Protocol A determines the dependence of the vulnerability results upon specific test conditions, and Protocol B determines the vulnerability curves referenced to shingle impact momentum. Protocol B was also used for the dowel experiments in Phase 3 (discussed later).

4.3. Phase 1 experimental details

The desired outcome of the shingle debris test program was to develop vulnerability curves quantifying the susceptibility of residential window glass to failure from shingle debris impact, referenced to impact momentum. The goal of Protocol A was to determine how dependent the identified momentum-to-damage thresholds are on the specific conditions of the debris impact test. For example, the vulnerability of 61 cm × 61 cm 3.18 mm thick (i.e. double-strength) annealed glass specimens impacted by 400 g shingles in a spinning flight mode may or may not be valid for 61 cm × 122 cm glass specimens, or smaller shingle debris, or tumbling shingles. Protocol A, used for Phase 1 only, determines the degree to which the vulnerability is dependent upon these specific test conditions, and thus the generalized applicability of the vulnerability curves produced by Phase 2 using Protocol B.

Table 1
Example of test sequence on a 61 cm × 61 cm × 3.18 mm annealed glass panel using Protocol A.

Specimen	Shingle mass (g)	RPM	Speed (m/s)	Damage
First pane	400	400	6.7	None
	400	450	7.6	None
	400	500	8.4	None
	390	550	9.2	None
	390	600	10.1	None
	405	650	10.9	None
	400	700	11.7	Shatter
New pane	400	700	11.7	None
	400	750	12.6	None
	400	800	13.4	Shatter
New pane	400	800	13.4	Shatter

Protocol A was designed to determine the minimum speed of a given shingle size/weight/flight mode necessary to crack or shatter glass specimens of given thickness/size. One test sequence consisted of failing multiple glass specimens. The first specimen was impacted starting at a low speed (6.71 m/s), then the tests were repeated using incrementally larger velocities until a crack or shattering occurred. Upon failure, the glass was replaced with a new specimen of the same thickness and size. The first impact on the new specimen was conducted at the speed that caused breakage of the first specimen. If the new specimen broke at first impact, that test sequence was deemed complete. If the new specimen did not break, the speed was incrementally increased until breakage occurred, and a third specimen was tested starting at the breaking speed of the second specimen. This process was continued as necessary (a fourth specimen, etc.) until a specimen broke from the first impact at the speed of damage from the previous specimen. Table 1 demonstrates a single test sequence for 61 cm × 61 cm double-strength annealed glass impacted by a 400 g shingle in spinning flight. The sequence in Table 1 required three specimens to complete, but sequences required between two and five specimens until the final specimen broke at first impact at the breaking speed of the previous specimen. A shingle was replaced if it was damaged during a test.

Data from the first-impact breakage specimen (the last specimen in any given sequence) was not used in the compiled results

Table 2
Results matrix for Test Protocol A (Phase 1). Mean breaking speed, momentum and kinetic energy.

ID number	1	2	3	4	5	6	7
# Specimens tested	12	15	13	7	6	6	9
Impact angle	90°						
Shingle type	New full	New half	Old full	Old half	New full		
Flight mode	Spinning				Tumbling	Spinning	
Glass thickness (mm)	3.18						4.76
Glass dim. (cm)	61 × 61	61 × 61	61 × 61	61 × 61	61 × 61	61 × 122	61 × 61
Shingle speed (m s^{-1})	12.31	21.11	14.07	19.83	11.04	12.31	18.09
Momentum (kg m s^{-1})	4.91	4.31	5.38	4.03	4.50	4.94	7.15
Momentum CoV	0.20	0.231	0.263	0.224	0.140	0.136	0.102
Energy (kg m^2 s^{-2})	31.33	31.81	40.29	27.80	33.50	30.89	65.21
Mean momentum of all 593.18 mm glass specimens = 4.72 kg m s^{-1}, CoV = 0.23							

Table 3
Results of ANOVA and Welch's *t* tests on Protocol A (Phase 1).

ID number pair	1/6	1/7	1/5	1/3	2/4	1/2	3/4
Description	61 × 61 versus 61 × 122	3.18 mm versus 4.76 mm	Spinning versus Tumbling	New full versus Old full	New half versus Old half	New full versus New half	Old full versus Old half
ANOVA *p* value	0.93	1.5E−05	0.37	0.34	0.53	0.14	0.04
Welch's *t* test *p* value	0.93	8.9E−06	0.30	0.33	0.52	0.14	0.02
Same mean 95% significance	Yes	No	Yes	Yes	Yes	Yes	No

statistics, as the 'minimum' momentum to damage was not determined for that specimen. Multiple test series were conducted for a given shingle type/size/weight, and given glass thickness and size, to provide a statistical assessment of the minimum momentum-to-damage threshold.

4.3.1. Phase 1 variables

Tests were conducted on three annealed glass specimen sizes: 61 cm × 61 cm 3.18 mm thickness, 61 cm × 122 cm 3.18 mm thickness, and 61 cm × 61 cm 4.76 mm (3/16 in) thickness, each restrained (using a continuous clamp) along the top and bottom of its edges. The 61 cm × 122 cm specimen was restrained along the short sides. The angle of impact was 90° for all tests.

Both new and aged three-tab shingles were used as debris, in "half" and "full" sizes. A full-size shingle is a 30.5 cm × 30.5 cm (12 in × 12 in) single tab, nominally weighing 400 g. Half-size shingles are cut from a single tab to 21.6 cm × 21.6 cm (8.5 in × 8.5 in), nominally weighing 200 g. Specimens were cut from a three-tab asphalt composite fiberglass Class F shingle product. Old shingles are more brittle than new shingles, and may affect momentum transfer to the glass upon impact. Thus, old shingles were recovered from a contractor reroofing a property in Florida (estimated age of 20 years).

All four shingle types were tested in the spinning flight mode. Full-size new shingles were also tested in tumbling flight mode. During Phase 1, a total of 68 glass specimens were tested to failure, excluding the first-impact breaking specimens (e.g. last row of Table 1).

4.3.2. Phase 1 results

Table 2 presents the average velocity, momentum and kinetic energy thresholds of breakage for shingle impacts perpendicular to the plane of the glass specimen. The following observations were made.

- Impact momentum is a more consistent threshold value than kinetic energy, which justifies developing vulnerability curves referenced to impact momentum.
- The mean debris impact momentum damage threshold is clearly higher for 4.76 mm glass (ID number 7 in Table 2) when compared to tests on 3.18 mm glass (ID numbers 1–6).
- Mean momentum damage threshold values among tests on 3.18 mm glass with various shingle sizes, ages, and flight modes (ID 1–6) appear similar. Combining tests on all 3.18 mm glass specimens produces an overall mean momentum value of 4.71 kg m/s, with a coefficient of variation (CoV) of 0.23.
- Mean momentum values for various 3.18 mm glass tests require statistical testing to reveal the significance of similarities and differences.

The one-way ANOVA test [40] was utilized to determine the statistical similarity between the mean breakage momentums among pairs of tests. The Welch's *t* test with unequal variance was also applied [41], since the ANOVA requirement of equality of variance among tested groups is not strictly accurate for these data. For both tests, a *p* value that exceeds 0.05 supports the hypothesis of equal means with a significance level of 95%. Values of *p* closer to 1.0 show stronger support of the equal mean hypothesis than values closer to 0.05.

Table 3 presents the results of the ANOVA and Welch's *t* tests conducted on seven pairs of results. The ID number assigned in Table 2 is used to identify the pairs tested in Table 3. For all pairs analyzed, only one controlled variable differed between the two tests, as noted in the Description row.

The breakage momentum of each specimen is used in the analyses. For example, the tests on ID pair 1 versus 6 (denoted 1/6 in Table 3) use all 12 breakage momentum values from tests in ID 1, and all six breakage momentum values from tests in ID 6 to determine whether the damage momentum from spinning new full-size shingles impacting 3.18 mm thick 61 cm × 61 cm specimens differs from those of 61 cm × 122 cm specimens (all other control variables identical). In this case, the *p* value for both tests, reported in Table 3 as 0.93, indicates a high degree of confidence that the mean breaking momentum of the two specimen sizes is statistically the same. This is indicated in Table 3 in the 'Same mean' row.

The following observations are made based on Table 3.

- Specimen size (ID pair 1 versus 6): The minimum momentum to damage appears not to be a function of glass pane area, which justified the continued use of 61 cm × 61 cm specimens in Phases 2 and 3. However, this conclusion cannot be extended to glass samples of significantly larger size absent additional

Table 4
Phase 2: Results from M_1 test sequence for spinning shingles at 90° impact angle.

Specimen	$M_1 = 4.7$ kg m/s	$M_2 = 5.4$ kg m/s	$M_3 = 5.7$ kg m/s	$M_4 = 6.0$ kg m/s	$>M_4$
O—no breakage X—breakage					
1	O	O	O	X	
2	X				
3	O	O	X		
4	O	O	X		
5	O	X			
6	O	O	O	X	
7	X				
8	O	X			
9	O	X			
10	O	O	X		
11	O	O	O	O	9.9 kg m/s
12	O	O	X		
13	O	O	O	X	
14	O	X			
15	O	O	O	O	6.9 kg m/s
16	O	O	O	X	
17	O	O	O	O	6.7 kg m/s
18	O	X			
19	O	O	X		
20	O	O	X		

testing. Thus the damage thresholds found in Phases 2 and 3 are not likely to be accurate for larger glass specimens more typical of commercial applications.

- Specimen thickness (ID pair 1 versus 7): The difference in the momentum threshold is significant when comparing 3.18 mm to 4.76 mm specimens. Applying the limiting case of zero thickness supporting zero momentum, the thickness (0, 3.18, 4.76 mm) and momentum (0, 4.91, 7.15 mm) data points describe a linear relationship between the thickness and the momentum threshold.
- Flight mode (ID pair 1 versus 5): The tumbling flight mode produced a lower mean value of damage momentum compared to the spinning mode. The means are the same with a 70% significance level ($1 - 0.30$ p value). High speed footage of shingle impact in both flight modes reveals that the tumbling shingle tends to damage the glass via slapping of the shingle against the glass (Fig. 2). This is not observed for the spinning shingles, which tend to crumple upon impact (Fig. 3).
- Shingle age (ID pairs 1 versus 3 and 2 versus 4): There is no consistent difference in momentum threshold when comparing old and new shingles. Old full-size shingles required a higher mean momentum than new full-size shingles. For half-size shingles, old shingles required less momentum than new shingles. In both cases the means are statistically the same.
- Shingle size (ID pairs 1 versus 2 and 3 versus 4): There is a consistent difference in threshold momentum when comparing full-size shingles to half-size shingles. New half-size shingles require less momentum on average than new full-size shingles. The statistical tests support the same mean hypothesis, but not strongly. Old half-size shingles require less momentum on average than old full-size shingles. The statistical tests do not support the same mean hypothesis.

4.4. Phase 2 experimental details

Phase 2 was designed to produce vulnerability curves relating the probability of breakage to full-size new shingle impact momentum. In order to evaluate the effect of accumulated damage from repeated impacts, each test specimen was impacted at predetermined increasing speeds until breakage occurred. The protocol began by identifying a series of momentum values at which testing would be conducted. For any given set of fixed test variables, a calibration round of testing on 20 glass specimens was first conducted. Each of the 20 specimens was impacted at increasing momentum values until failure occurred. The data from this calibration round was used to project a rough estimate (ignoring damage accumulation) of the impact momentum expected to damage 20%, 40%, 60%, and 80% of the tested samples upon first impact, denoted M_1 through M_4. A test sequence of 20 specimens was then conducted for M_1 through M_4.

The M_1 test sequence began with a specimen subjected to impact momentum M_1. If no damage occurred, that same specimen was impacted at M_2, and so on, until the specimen broke. If no damage occurred by M_4, higher momentum values were used until breakage. This was repeated for 20 specimens, each with first impact at M_1. Table 4 provides the results of the M_1 test sequence, where 'O' indicates an impact with no breakage, and 'X' indicates an impact with breakage. The M_2 test sequence followed the same procedure, with first impact at momentum M_2 and proceeding to M_3, M_4, and higher until breakage. Thus the M_2 test sequence would have no data in column M_1 of Table 4.

The results from the first-impact tests (column M_1 for sequence M_1, column M_2 for sequence M_2, etc.) were utilized to construct the first-impact vulnerability curve. The results from impacts after the first impact (i.e. accumulated impact) were analyzed to quantify the distribution of momentum thresholds for specimens experiencing more than one impact.

4.4.1. Phase 2 variables

Phase 2 specimens had dimensions of 61 cm × 61 cm × 3.18 mm and were restrained along all four edges. Only new full-size shingles (30.5 cm × 30.5 cm 400 g) were used as debris.

Test Protocol B was conducted for three different sets of control variables, producing three first-impact vulnerability curves. The spinning shingle flight mode was conducted at 45° and 90° angles of impact, and the tumbling flight mode was conducted at

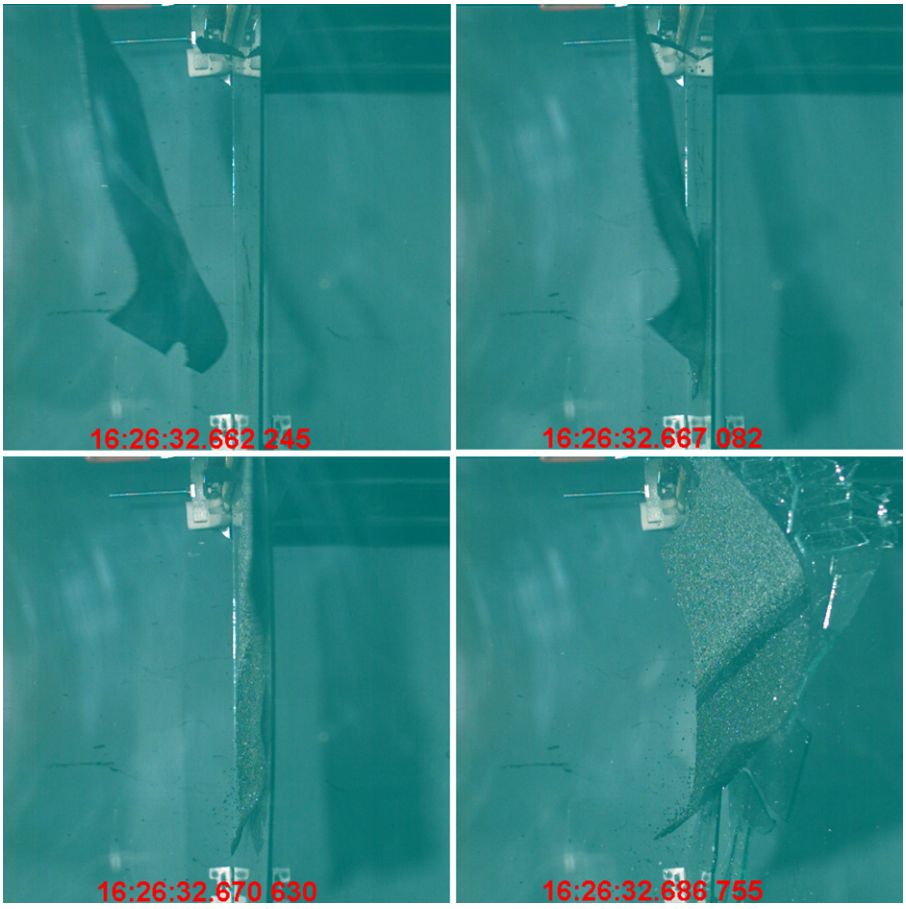

Fig. 2. High speed imagery of a tumbling shingle impact (Phase 1 testing).

90° angle of impact. For both spinning test series, the first-impact results differed significantly from the results from the calibration test round, which indicated a significant influence of damage accumulation. This prompted an additional two sequences of 20 specimen tests at higher first-impact momentum values for both the 45° and 90° spinning impact test series. A total of 320 glass specimens were tested to failure to complete the three first-impact vulnerability curves from Phase 2 shingle impact testing.

4.4.2. Phase 2 results

Fig. 4 illustrates the first-impact vulnerability results for spinning shingles at 90° impact, spinning shingles at 45° impact, and tumbling shingles at 90° impact. Each data point represents the percentage of 20 samples that broke upon first impact at a given momentum. For example, column M_1 of Table 4 provides the 10% value at the lowest momentum for spinning shingle 90° impact results in Fig. 4.

The 95% confidence interval for first-impact results is included in Fig. 4. If a given test sequence of 20 specimens (one data point in Fig. 4) was repeated many times, the confidence interval represents the range in which the percentage-damaged results are expected to fall for 95% of these 20 specimen sequences. The confidence intervals were calculated using the adjusted Wald method [42,43], assuming that the outcome from any 20 specimens is binomially distributed (a sum of Bernoulli samples). This requires that any first-impact test has two possible outcomes (break or non-break) and is independent of the impact results on other specimens. Both of these conditions meet the established protocol. The 95% confidence interval was also calculated using a simple Monte Carlo simulation of Bernoulli random variables (not shown), which closely conformed to the intervals calculated using the adjusted Wald method presented in Fig. 4.

Table 5
Phase 2: Accumulated shingle impact analysis.

	Spin 90	Spin 45	Tumble 90	Combined
Breaking momentum (kg m s^{-1})				
Mean	6.4	7.1	5.6	6.5
CoV	0.13	0.13	0.08	0.15
No. of impacts before break				
Mean	3	3.1	1.75	2.80
CoV	0.79	0.55	0.67	0.71
Range	[1, 14]	[1, 7]	[1, 6]	[1, 14]

The results indicate that glass has a lower damage momentum threshold for shingle debris in a tumbling flight mode, which is consistent with the results from Phase 1. More deformation of the spinning shingle provides a less elastic collision and less momentum transfer to the glass (Figs. 2 and 3).

The angle of debris impact also influences the transfer of momentum to the glass. In Fig. 4, the 45° impact corresponds to lower percentage damage than 90° for a given momentum.

Vulnerability curves such as those in Fig. 4 are not provided for the accumulated-impact data. The accumulated-impact test protocol produced impacts whose outcome was not independent from other impacts, since any given glass specimen was impacted at least twice, and as many as 15 times at increasing speeds until the specimen broke. The absence of this independence among impacts and the consistency of the number of impacts render an accumulated-impact vulnerability curve less meaningful.

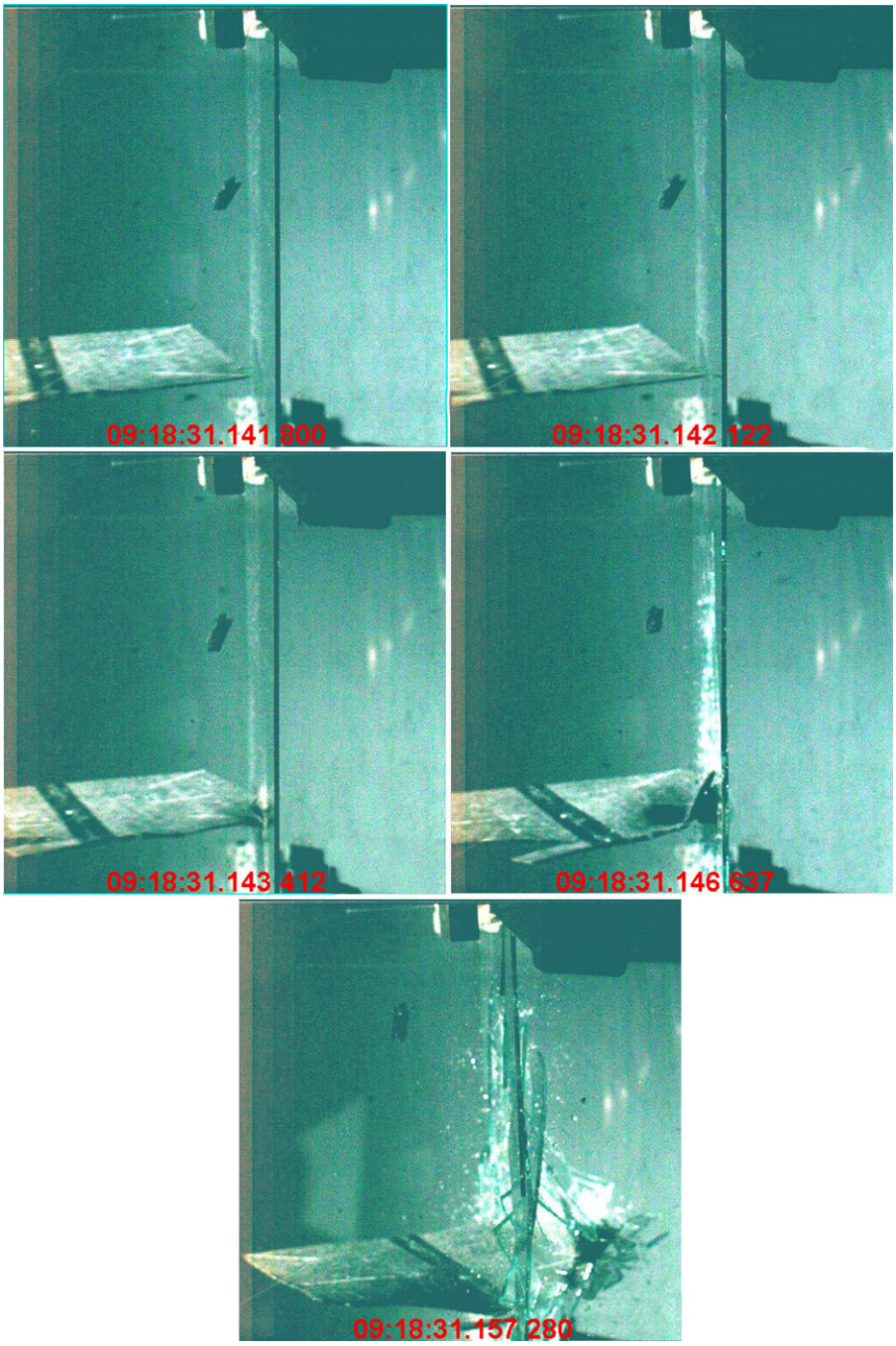

Fig. 3. High speed imagery of a spinning shingle impact (Phase 1 testing).

The accumulated-impact results are presented in Table 5 as the mean and coefficient of variation of breaking impact momentum, mean and coefficient of variation of the number of impacts prior to breaking, and the range of number of impacts needed to break specimens. Fig. 5 presents the normalized histograms of the accumulated-impact breaking momentum values summarized in row one of Table 5. It can be observed that the glass specimens that survived the first impact on average required one or two additional impacts before breaking. A few outliers required considerably more impacts, leading to the high CoV in row four of Table 5. Consistent with the first-impact and Phase 1 results, the damage threshold for the tumbling flight mode is lower than that of the spinning mode.

The accumulated-impact results in Table 5 may be compared with the results from Phase 1 testing in Table 2. The new full-size spinning shingle and tumbling shingle results (ID numbers 1 and 5 in Table 2) have mean momentum threshold values of 4.91 and 4.50 kg m/s, respectively. In Table 5, the corresponding threshold values are 6.4 and 5.6 kg m/s. The only difference between the experimental configurations for Phases 1 and 2 was the use of a two-sided specimen restraint in Phase 1 and a four-sided restraint in Phase 2.

4.4.3. Phase 2 discussion

The first-impact and accumulated-impact results from Phase 1 and Phase 2 testing indicate that a shingle momentum of 10 kg m/s yields a very high probability of damage to unprotected 3.18 mm annealed glass. For the 400 g shingles used in Phase 2, this corresponds to a speed of 25 m/s. Recently, researchers at the University of Western Ontario Boundary Layer Wind Tunnel Laboratory found

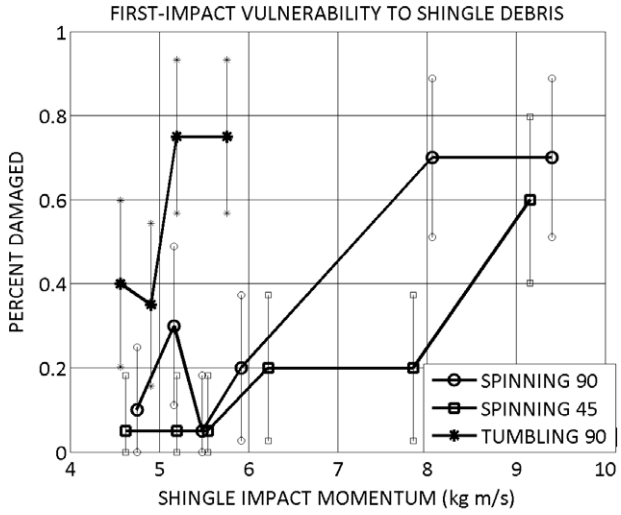

Fig. 4. First-impact vulnerability results for shingle impact on 3.18 mm annealed glass. Each marker represents the percentage damaged out of 20 specimens. 95% confidence interval included.

that the flight speed of shingles released from a residential rooftop of common slope can range from 50% to 120% of the roof height gust speed as measured without the house model present [39]. Thus a shingle traveling at 50% of the gust wind speed would require a gust of 50 m/s to achieve a momentum with a greater than 70% probability (see Fig. 4) of damaging double-strength annealed residential window glass. Converting an open exposure three second gust to marine exposure one minute sustained wind using a factor of 0.9 [44] results in a Category 2 hurricane intensity on the Saffir–Simpson Hurricane Scale. Post-storm observations indicate significant shingle loss begins to occur typically in Category 2 winds. Using these same assumptions, a minimal Category 1 wind intensity will impart a momentum of 7.5 kg m/s to a 400 g loose shingle, corresponding to ∼50% probability of breaking double-strength annealed glass (the frequency of such an impact occurring is not addressed here). Therefore, winds strong enough to remove shingles from a rooftop are highly likely to impart a momentum to that shingle sufficient to break a typical residential double-strength window pane.

5. Simulation of dowel impacts (Phase 3)

5.1. Description of testing apparatus

The launching apparatus was designed to propel wooden oak dowels over a short distance into a glass specimen. An air cannon accelerates the projectile down a 4 m PVC barrel (Fig. 6). Barrel sizes were made with 2.54 cm to 6.35 cm diameter PVC, in 1.27 cm increments, to accommodate a range of dowel sizes. A ball valve was inserted between the air tank and the barrel to allow computer control dowel firing. NI Labview 8.5 Software was used to measure the pressure of the tank and receive start and stop pulses from two pair of through-beam photoelectric sensors. A distance of 15.24 cm between the sensors was divided by the time interval recorded by the device to determine the missile velocity.

For low velocity tests, it became evident we could not obtain sufficient precision with the air cannon apparatus. Therefore, a drop-test apparatus was designed to accelerate the dowel to a specific velocity based on the height of the drop. The impact location and angle of impact can be changed by rotating and tilting the test apparatus as required.

A glazing support frame and fragment containment box were constructed with dimensions and fittings identical to those described for the shingle testing (see Section 4.1). This parallel system allowed both shingle and dowel testing to be conducted concurrently.

The dowels were created from freshly cut live oak tree limbs recovered from a tree recycling facility in Gainesville. The rough limbs range from 12 to 15 cm in diameter, and were lathed into 2.54 and 5.08 cm diameter dowels weighing 200 g. The moisture content of the freshly cut limbs ranged from 30% to 40%. Any given dowel was only used for a 24 h period after machining to maintain natural moisture level. If the weight of the dowel changes by more than 10 g from its original weight, it was replaced prior to that 24 h period.

5.2. Testing protocol

The test protocol is identical to Protocol B used in Phase 2.

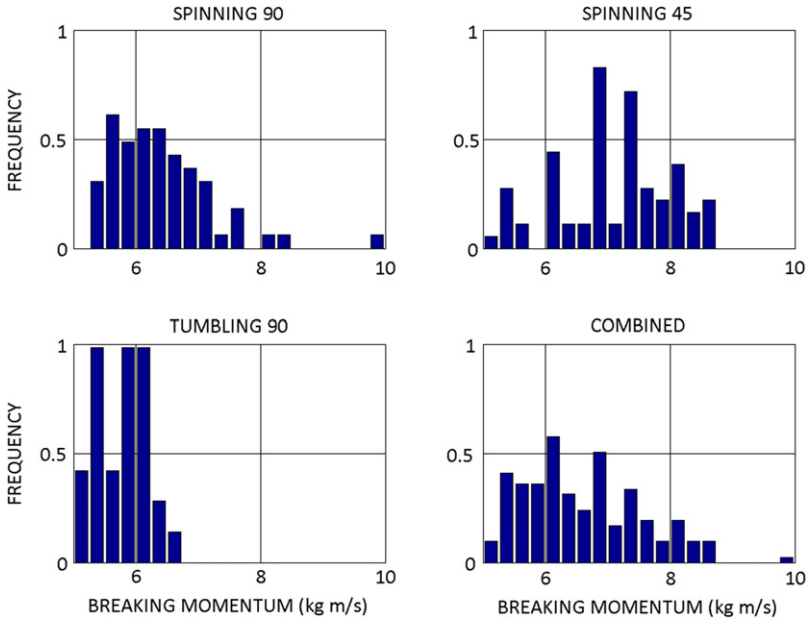

Fig. 5. Normalized histogram of shingle accumulated-impact breaking momentum.

Fig. 6. Dowel launcher and glazing mounts for air cannon and drop test apparatus.

5.3. Phase 3 variables

Only 61 cm × 61 cm double-strength glass specimens were tested for Phase 3 and were restrained (using a continuous clamp) along all four edges. A calibration round and multiple test sequences were conducted for two different sets of control variables: 5.04 cm diameter 200 g dowels at 90° angle of impact, and 2.54 cm diameter 200 g dowels at 90° angle of impact. A third set of control variables, 5.04 cm diameter 200 g dowels at 45° angle of impact, was applied for two test sequences. A total of 260 glass specimens were tested to failure to complete the three first-impact vulnerability curves for Phase 3 dowel impact testing.

5.4. Phase 3 results

Fig. 7 shows the first-impact vulnerability results for 2.54 cm diameter dowels at 90° impact, 5.08 cm diameter dowels at 90° impact, and 5.08 cm diameter dowels at 45° impact. The ordinate is the percentage of 20 samples that broke upon first impact. The 95% confidence interval for first-impact results is included in Fig. 7 using the adjusted Wald method [42,43]. The trends in the data indicate that close to 100% first-impact failure is expected between 3 and 4 kg m/s for both dowel diameters at 90° impact. As was the case with shingles, the 45° impact vulnerability requires higher momentum to achieve failure rates comparable to the 90° impact results. Achieving results for larger momentums was not possible for the 45° tests, as the back end of the dowels began fracturing by impacting the test frame.

The accumulated-impact results are presented in Table 6 as the mean and coefficient of variation (CoV) of breaking impact momentum, mean and coefficient of variation of the number of impacts prior to breaking, and the range of number of impacts needed to break specimens. Fig. 8 presents the normalized histograms of the accumulated-impact breaking momentum values summarized in row one of Table 6. It can be observed that the glass specimens that survived the first impact on average required one or two additional impacts before breaking. A few outliers required considerably more impacts before breaking, leading to the large CoV in row four of Table 6.

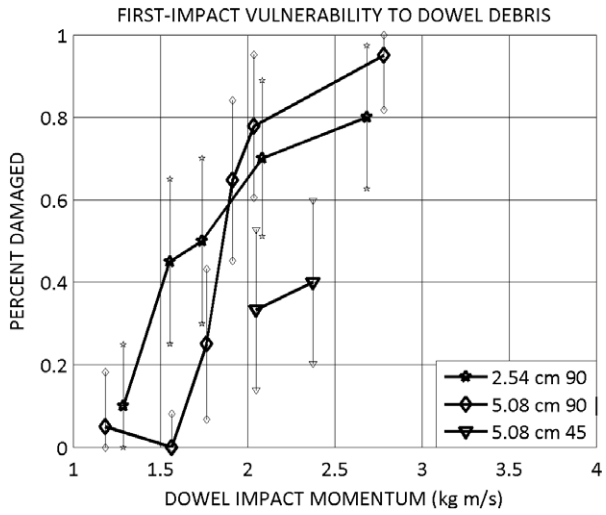

Fig. 7. First-impact vulnerability results for dowel impact on 3.18 mm annealed glass. Each marker represents the percentage damaged out of 20 specimens. 95% confidence interval included.

5.5. Phase 3 discussion

The first-impact and accumulated-impact results from Phase 3 testing indicate that a dowel momentum of 4 kg m/s yields a very high probability of damage to unprotected double-strength annealed glass (Fig. 7). For the 200 g dowels used in all tests, this corresponds to a speed of 20 m/s. Given the variety of possible geometries, foliage, etc., documentation on the gust wind speed

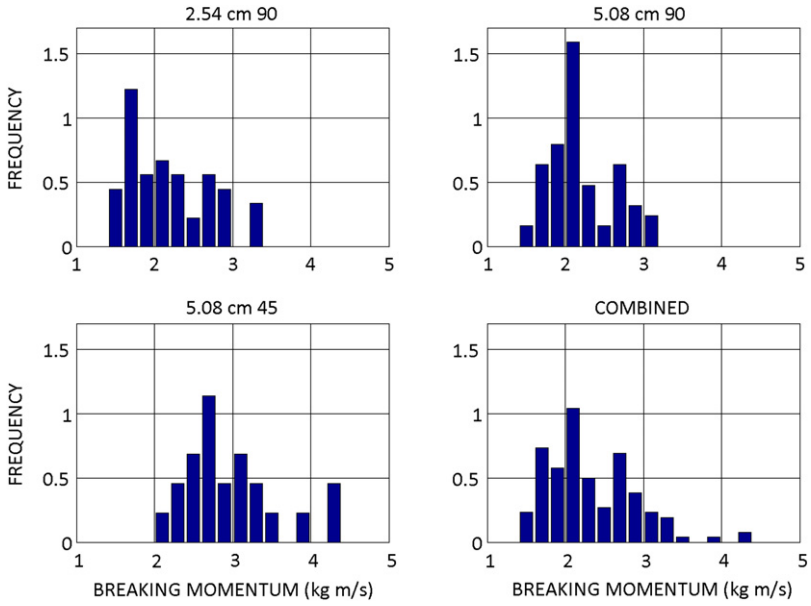

Fig. 8. Normalized histogram of dowel accumulated-impact breaking momentum.

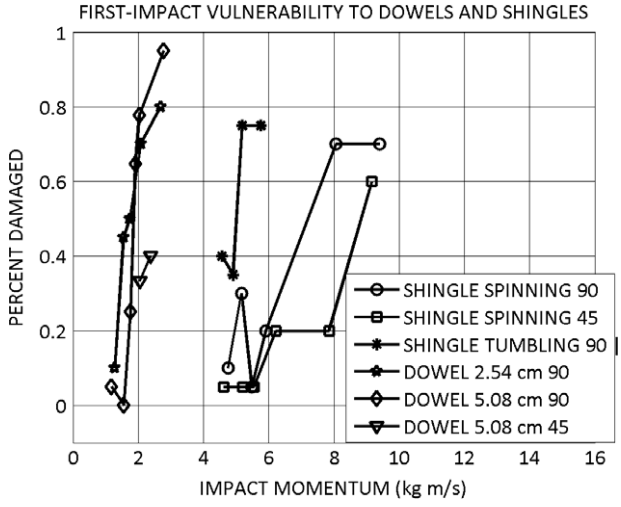

Fig. 9. First-impact vulnerability results for shingle and dowel impacts on 3.18 mm annealed glass. Figs. 4 and 7 combined.

Table 6
Phase 3: Accumulated dowel impact analysis.

	2.54 cm 90	5.08 cm 90	5.08 cm 45	Combined
Breaking momentum (kg m s^{-1})				
Mean	2.20	2.22	2.98	2.34
CoV	0.23	0.18	0.20	0.24
No. of impacts before break				
Mean	2.58	3.64	2.64	3.11
CoV	0.57	0.61	0.66	0.63
Range	[1, 6]	[1, 8]	[1, 7]	[1, 8]

necessary to propel 200 g vegetation at 20 m/s is not available to our knowledge. Applying an assumption that the vegetation will travel at 40% of the gust speed that releases the debris, results in a 50 m/s gust, or Category 2 sustained winds. Under these same assumptions a minimal Category 1 local wind field is capable of imparting a momentum of 3 kg m/s, corresponding to over 80% probability of failure for 90° impact.

Fig. 9 provides the first-impact vulnerability results from both Phase 2 shingle and Phase 3 dowel testing in the same plot for convenient comparison. Shingle debris requires significantly higher momentum to damage the glass specimen. This result is expected given that the dowels undergo almost no deformation upon impact, imparting more energy to the glass specimen compared with highly deformable shingles impacting at the same momentum.

6. Conclusions

Testing was conducted to quantify the vulnerability of double-strength annealed glass to shingle and dowel impacts. Shingles and dowels were selected as windborne debris commonly observed in post-hurricane damage investigations, and represent a significant source of damage to residential glazing. Custom launching apparatuses were constructed to achieve controllable and repeatable flight modes and speeds for the debris. More than 600 annealed residential window glass specimens were tested to determine momentum threshold and damage accumulation. Vulnerability curves are provided for unprotected window glass as a function of momentum, debris type, flight mode, and angle of impact.

For both shingles and dowels, debris weighing between 200 and 400 g would very likely achieve momentum sufficient to break unprotected double-strength annealed glass if the local wind field is of low Category 2 intensity on the Saffir–Simpson Hurricane Scale. Category 1 wind speeds are capable of imparting momentum with a significant probability of breakage. These conclusions as well as the specific thresholds identified cannot be extended to double-strength annealed glass specimens of significantly larger dimensions or different boundary conditions than those used in this study. For example, some commercial applications utilize much larger spans, and this may change the impact dynamics, glass response, and overall momentum threshold.

This paper specifically addresses the conditional probability (severity) of lightweight debris impact damaging residential glass. In the context of hazard modeling, these study results must be coupled with a separate evaluation of the likelihood of debris impact occurring.

Acknowledgements

The authors thank the Florida Building Commission for sponsoring this research. The contributions of Mr. Jim Austin and Mr. Scott Bolton are gratefully acknowledged.

References

[1] ASTM E1886-05. Standard test method for performance of exterior windows, curtain walls, doors, and storm shutters impacted by missile(s) and exposed to cyclic pressure differentials. West Conshohocken (PA): American society for testing and materials, 100 Barr Harbor Drive, PO Box C700, 19428.

[2] TAS 201-94. Impact test procedures. Florida building code test protocols for high-velocity hurricane zones. Tallahassee (Florida): Department of community affairs building codes and standards, 2555 Shumard Oak Boulevard, 32399.

[3] AAMA 506-05. Voluntary specification for hurricane impact and cyclic testing of fenestration products. Schaumburg (Illinois): American architectural manufacture association, 1827 Walden office square, Suite 550. 60173-4268. 2005.

[4] Minor J. Windborne debris and building envelope. J Wind Eng Ind Aerodyn 1994;53(1–2):207–27.

[5] Vickery PJ, Skerlj PF, Lin J, Twisdale Jr LA, Young MA, Lavelle FM. HAZUS-MH hurricane model methodology. II: Damage and loss estimation. Nat Hazards Rev 2006;7(2):94–103.

[6] Pita GL, Pinelli J-P, Gurley K, Weekes J, Subramanian CS, Hamid S. Vulnerability of mid-high rise commercial–residential buildings in the Florida Public Hurricane Loss Model. In: Proceedings European safety and reliability conference ESREL. 2009.

[7] Gurley K, Davis R, Ferrera S-P, Burton J, Masters F, Reinhold T. et al. Post 2004 hurricane field survey—An evaluation of the relative performance of the standard building code and the Florida building code. St. Louis: ASCE structures congress; 2006.

[8] Federal emergency management agency (FEMA). Washington (DC): Mitigation assessment team report: Hurricane Charley in Florida rep. no. FEMA 488. 2005. p. 5.1–68.

[9] Federal emergency management agency (FEMA). Washington (DC): Mitigation assessment team report: Hurricane Ivan in Alabama and Florida rep. no. FEMA 489; 2005. p. 5.1–65.

[10] Meloy N, Sen R, Pai N, Mullins G. Roof damage in new homes caused by Hurricane Charley. J Struct Eng 2007;21(2):97–107.

[11] Brungs MP. Fracture and failure of glass. Mater Forum 1995;19:227–39.

[12] Beason WL, Meyers GE, James RW. Hurricane related window glass damage in Houston. J Struct Eng 1984;110(12):2843–57.

[13] Oliver C, Hanson C. In: Cook RA, Soltani M (Eds.), Failure of residential building envelopes as a result of Hurricane Andrew in Dade County. Florida hurricanes of 1992; p. 496–508.

[14] Ayscue JK. Hurricane damage to residential structures: Risk and mitigation 1996. Retrieved October 20, 2008 from natural hazards research and applications information center. http://www.colorado.edu/hazards/publications/wp/wp94/wp94.html.

[15] Beason WL. Breakage characteristics of window glass subjected to small missile impacts. Thesis. Civil Engineering Department. Texas Tech University; 1974.

[16] Harris PL. The effects of thickness and temper on the resistance of glass to small missile impact. Thesis. Civil Engineering Department, Texas Tech University; 1978.

[17] Pantelides CP, Horst AD, Minor JE. Post breakage behavior of heat strengthened laminated glass under wind effects. J Struct Eng 1993;119(2):454–67.

[18] Behr RA, Kremer PA. Performance of laminated glass units under simulated windborne debris impacts. J Archit Eng 1996;2(3):95–9.

[19] Ji FS, Daharani LR, Behr RA. Damage probability in laminated glass subjected to low velocity small missile impacts. J Mater Sci 1998;33(19):4775–82.

[20] Saxe TJ, Behr RA, Minor JE, Kremer PA, Dharani LR. Effects of missile size and glass type on impact resistance of sacrificial ply' laminated glass. J Archit Eng 1992;8(1):24–39.

[21] Dharani LR, Ji F, Behr RA, Minor JE, Kremer PA. Breakage prediction of laminated glass using the sacrificial ply design concept. J Archit Eng 2004;10(4):126–35.

[22] Minor JE. Window glass in windstorms. Civil engineering report series CE 74-01, Texas Tech University, Lubbock, Texas; 1974.

[23] NAHB research center. WindBorne debris—Impact resistant of residential glazing. Report prepared for the US Department of housing and Urban development 2002. Partnership for advancing technology in housing—PATH program.

[24] Minor JE. Window glass failures in windstorms. ASCE J Struct Div 1976;102:147–60.

[25] Bole SA. Investigations of the mechanics of windborne missile impact on window glass. Thesis. Civil Engineering Department, Texas Tech University; 1999.

[26] Ball A, McKenzie HW. On the low velocity impact behavior of glass plates. J Physique 1994;IV4(8): c8-783–8.

[27] Wilson JF. Similitude experiments on projectile induced fracture of monolithic glass. Int J Impact Eng 1996;18(4):417–24.

[28] Wiederhorn SM, Lawn BR. Strength degradation of glass impacted with sharp particles: I. Annealed surfaces. J Am Ceram Soc 1979;62(1–2):66–70.

[29] Twisdale LA, Vickery PJ, Steckley AC. Analysis of hurricane windborne debris risk for residential structures. Raleigh (NC): Applied Research Associates Inc.; 1996.

[30] HAZUS-MH Technical Manual, Washington (DC): Federal Emergency Management Agency (FEMA); 2003.

[31] Lin N, Vanmarcke E. Windborne debris risk assessment. Probabilist Eng Mech 2008;23:523–30.

[32] Wills JAB, Lee BE, Wyatt TA. A model of windborne debris damage. J Wind Eng Ind Aerodyn 2002;90(4–5):555–65.

[33] Holmes JD. Wind loading of structures. New York (NY): Spon Press; 2002.

[34] Holmes JD. Trajectories of spheres in strong winds with application to wind-borne debris. J Wind Eng Ind Aerodyn 2004;92(1):9–22.

[35] Tachikawa M. A method for estimating the distribution range of trajectories of wind-borne missiles. J Wind Eng Ind Aerodyn 1988;29(1–3):175–84.

[36] Lin N, Letchford CW, Holmes JD. Investigations of plate-type windborne debris. Part I. Experiments in wind tunnel and full scale. J Wind Eng Ind Aerodyn 2006;94(2):51–76.

[37] Lin N, Holmes JD, Letchford CW. Trajectories of windborne debris and applications to impact testing. ASCE J Struct Eng 2007;133(2):274–82.

[38] Holmes JD, Letchford CW, Lin N. Investigations of plate-type windborne debris. II. Computed trajectories. J Wind Eng Ind Aerodyn 2006;94(1):21–39.

[39] Kordi B, Kopp GA. The effect of local flow field on the flight on wind-borne debris. In: 11th Americas conference on wind engineering. 2009.

[40] Hogg RV, Ledolter J. Engineering statistics. New York: MacMillan; 1987.

[41] Welch BL. The generalization of "student's" problem when several different population variances are involved. Biometrika 1947;34:28–35.

[42] Agresti A, Coull B. Approximate is better than 'exact' for interval estimation of binomial proportions. Amer Statist 1998;52:119–26.

[43] Sauro J, Lewis J. Estimating completion rates from small samples using binomial confidence intervals: Comparisons and recommendations. In: Proceedings of the human factors and ergonomics society. 49th annual meeting. 2005. p. 2100–4.

[44] Simiu E, Vickery PJ, Kareem A. Relation between Saffir–Simpson Hurricane Scale wind speeds and peak 3-s gust speeds over open terrain. ASCE J Struct Eng 2009;133(7):1043–5.